Sensor phenomena

Textile-Integrated Organic Electrochemical Transistor for Selective Ion Detection via Electrical Impedance Spectroscopy

Antonio Altana[1,2], Bajramshahe Shkodra[1], Pietro Ibba[1*], Martina Aurora Costa Angeli[1], Moritz Ploner[1], Mattia Petrelli[1], Eva-Maria Korek[3], Paolo Lugli[1,2**], and Luisa Petti[1***]

[1] *Sensing Technologies Laboratory (STL), Faculty of Engineering, Free University of Bozen-Bolzano, 39100 Bozen, Italy*
[2] *Competence Centre for Mountain Innovation Ecosystems, Free University of Bozen-Bolzano, 39100 Bolzano, Italy*
[3] *School of Computation, Information and Technology, Technical University of Munich, 80333 Munich, Germany*
[*] *Member, IEEE*
[**] *Fellow, IEEE*
[***] *Senior Member, IEEE*

Manuscript received 31 May 2024; accepted 12 June 2024. Date of publication 14 June 2024; date of current version 20 June 2024.

Abstract—In this letter, we present a novel approach for the fabrication of a fully printed poly(3,4 ethyldioxythiophene)poly(styrenesulfunate)-based organic electrochemical transistor (OECT) on textile substrates, that serves as a selective cation sensor, thanks to the combination of both OECT and electrochemical impedance spectroscopy (EIS) response. In particular, the selectivity achieved relies on discerning ion diffusion dynamics at low frequencies during EIS measurements and coupling these with the variations in OECT response associated with ion concentration. Unlike existing literature, our sensor is fabricated using cost-effective techniques, is planar, integrated directly onto textiles, and operates without external gate electrodes. Employing the same device configuration for both OECT and EIS measurements (both methods with a high coefficient of correlation $R^2 = 89\%$ and $R^2 > 94\%$, respectively), we demonstrate its efficacy by characterizing the sensor across three different concentrations of potassium chloride and sodium chloride, establishing a comprehensive 3-D calibration space to extract the electrolyte composition in a concentration between 1.25 and 100 mM.

Index Terms—Sensor phenomena, bioimpedance, flexible sensor, organic electrochemical transistor (OECT), PEDOT, PSS, stretchable sensor, sweat analysis, wearable electronics.

I. INTRODUCTION

In recent years, wearable transistor-based biosensors [1], [2], offering noninvasive and continuous monitoring capabilities, have emerged as promising device platforms in various applications, ranging from environmental monitoring to personalized healthcare. Traditional ion sensors rely on membrane-based systems [3], [4], which typically complicate the fabrication process and require long conditioning steps [5] or output signal post-processing [6], while at the same time increasing the overall cost of fabrication. To address these challenges, researchers have explored membrane-less sensing platforms based on organic electrochemical transistors (OECTs) taking advantage of their unique signal amplification and electrochemical functionalities, thus enabling sensitive detection of a wide range of analytes based on different ion dynamics approaches. An interesting material, which serves as channel for OECT, is represented by poly(3,4 ethyldioxythiophene)poly(styrenesulfunate) PEDOT:PSS. The working principle of a PEDOT:PSS-based OECT is based on the dedoping of the semiconducting channel, caused by the penetration of the cations due to the application of a positive gate voltage [7]. The literature provides different approaches for membrane-less ion selective OECT sensors, either employing multiple devices configuration [8] or expensive and not scalable manufacturing processes on rigid substrates [9]. Tseng et al. [10] introduced the concept of combining electrical impedance spectroscopy (EIS) with OECT V_{off} analysis to obtain information on diffusion dynamics by analyzing low-frequency spectral data and thus discern ionic species without the need of a membrane. This concept was nevertheless also shown on a rigid substrate and with the use of an external gate electrode. These aspects prevent the use of the device as a wearable sensor to be incorporated into smart clothing.In this work, we propose to overcome existing limitations in the field, by utilizing a simple and scalable fabrication solution for the integration of PEDOT:PSS-based OECTs onto textiles, with the final aim of allowing ion-selective sensing in smart garments. Our approach involves printing OECTs on thermoplastic polyurethane (TPU) that are able to provide small features and consistent electrode spatial references [11]. To achieve selectivity, our sensing platform is based on different ion diffusion dynamics, allowing discrimination of target ions without additional membrane layers. This simplifies device fabrication and operation, making it suitable for widespread adoption in wearable technology.

Corresponding author: Pietro Ibba (e-mail: pietro.ibba@unibz.it).
Associate Editor: Hamida Hallil.
Digital Object Identifier 10.1109/LSENS.2024.3414851

II. MATERIALS AND METHODS

A. OECT Fabrication

The fabrication process flow, the schematic of the OECT, and a picture of the real device are shown in Fig. 1. Before printing, the TPU (Micromax Intexar TE-11 C) substrates were subjected to a thorough cleaning process using an air gun to remove leftover particles, followed by a preheating step at 130 °C for 30 min, which is crucial to induce thermal stress on the substrate before subsequent printing steps. A screen printing process was employed for the fabrication of the gate using Ag/AgCl ink (LOCTITE EDAG PE409), followed by the simultaneous printing of source, drain, and channel using a

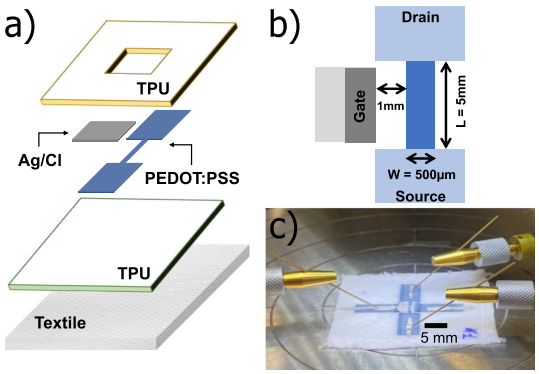

Fig. 1. Textile PEDOT: PSS OECT-based sensor. (a) Schematic of the structure. (b) Printed dimensions. (c) Picture of device while being characterized with a probe station and a parameter analyser.

PEDOT:PSS ink (5.0 wt.%, conductive screen printable ink from Sigma, film thickness ca. 2 µm), where the quality of the alignment between subsequent layers defines the channel gate distance, nominally 1 mm. The samples were cured in oven at 120 °C for 15 min after each printing step. Following, to integrate the TPU substrate onto the textile Crono (AP) (TEXmarket Srl), a heat press transfer method was employed [12], ensuring optimal conformal contact and stability. In the final step of fabrication, the channel area was defined by applying another layer of TPU as encapsulation.

B. Diffusion Characterization

One of the most used techniques for assessing the characteristic of an electrochemical system is cyclic voltammetry (CV). For the measurements, the PEDOT:PSS channel served as the working electrode (with source and drain electrodes short-circuited), a platinum wire as the counter electrode, and a Ag/AgCl electrode as the reference electrode, to decouple undesired interference from the other printed components. The ferricyanide/ferrocyanide ($[Fe(CN)_6]^{3-/4-}$) redox couple is the most common reversible redox system involving one electron transfer, which makes it an ideal redox couple for investigating the diffusion of redox species into the PEDOT:PSS channel [13]. Here, 5 mM of $Fe[(CN)_6]^{3-/4-}$ in 0.1 M potassium chloride (KCl) (at 25 °C) and applying different scan rates of 10, 20, 30, 40, 50, 60, 70, 80, and 90 mV/s, was used to investigate the diffusion phenomena of electroactive species in the PEDOT:PSS layer, as proposed in [14].

C. OECT Characterization

The OECT device underwent comprehensive electrical characterization through transfer characteristic measurements, in two different electrolyte solutions, namely, KCl and sodium chloride (NaCl) in water, each of them in three different concentrations (1, 10, and 100 mM). The transfer characteristics were recorded sweeping the gate-source voltage V_{GS}, 4 from −0.1 to 1 V, while maintaining the drain-source voltage V_{DS}, constant at −0.1 V. From the transfer characteristics, the response of the OECT to different V_{GS} was calculated as the variation of the drain current I_{DS} from the current I_{DS0} at $V_{GS} = 0.1$ V, namely, $(I_{DS} - I_{DS0})/ I_{DS0}$, as described in [15]. Specifically, the responseat a V_{GS} of 0.5 V was analyzed due to its significance in the device operation. At this working point, the PEDOT:PSS in the channel remains partially dedoped by the cations, leading to a measurable response that decreases with increasing ion concentration.

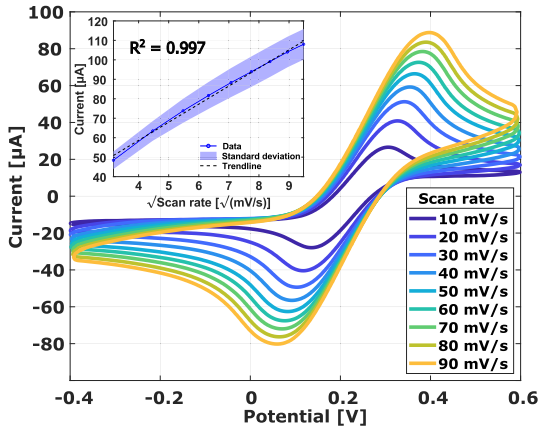

Fig. 2. Electrochemical behavior of PEDOT:PSS channel. CV responses in 5 mM of $[Fe(CN)_6]^{3-/4-}$ solution containing 0.1 M of KCl at different scan rates (10 to 100 mV/s), as well as linear correlation between the oxidation peak currents and the square root of the scan rates (inset).

D. EIS Characterizazion

For the EIS measurements, sinusoidal excitation of 50 mV amplitude was applied around the same operational point utilized for the OECT response analysis, employing a dc voltage of −0.5 V, at logarithmically spaced frequencies between 0.1 mHz and 10 kHz. The EIS measurements were performed employing the same NaCl and KCl solutions employed for the OECT characterization using the PEDOT:PSS as working electrode and the Ag/AgCl electrode as counter and reference, as in a two electrodes EIS measurement. To address the intrinsic variability in device dimensions arising from the printing process, the Nyquist plots obtained from EIS measurements were normalized, with reference to minimum and maximum values. The EIS data is typically modeled by using a Randles circuit including a Warburg element to model the diffusion process. To avoid the complexity of nonlinear data fitting, the resistance (R^*_W), as an indicator of different ion dynamics [10], was calculated from the intercept of the real component of the normalized impedance plot frequencies below 1 Hz. If ideal diffusion is considered (i.e., no double layer effects), this point of intersection indicates the diffusion resistance of the electrolyte [16], offering indications of both ion concentration and diffusion. Assuming the nonideality of the system, the value of R^*_W remains dependent on the ion concentration and includes the ion-specific details associated with diffusion constant [10].

III. RESULTS AND DISCUSSION

A. Diffusion Analysis

The PEDOT:PSS channel was studied in a standard redox system performing CV to investigate which phenomena affects the mass transfer process. In CV, the scan rate affects the kinetics of the redox reactions and the diffusion of species to and from the electrode surface. At higher scan rates, the diffusion layer becomes thinner [17], which facilitates faster mass transport, allowing electroactive species to reach the electrode surface more frequently and more quickly, resulting in elevated currents [18]. Such phenomenon is visible in Fig. 2, where increasing scan rates leads to higher peak currents. As shown in the graph, a good linear proportionality between the oxidation peak current and the square root of the scan rate is established (i.e., $R^2 = 99.76\%$, shown in the inset in Fig. 2), underlining that mass transfer is controlled by the diffusion [19].

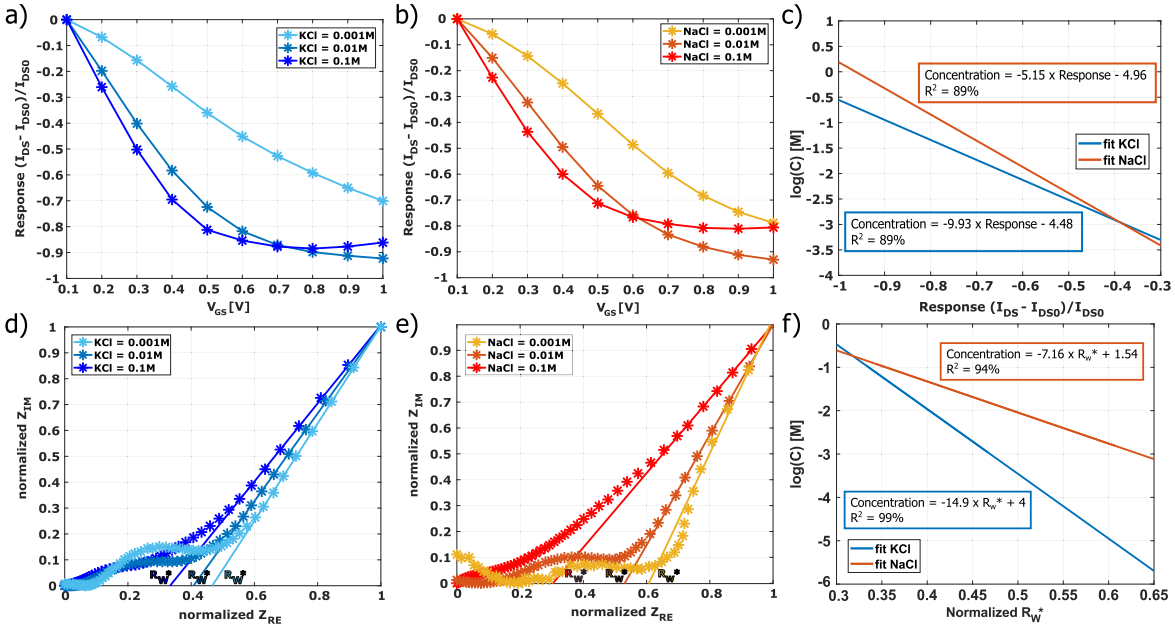

Fig. 3. OECT response toward (a) different KCl concentrations, (b) different NaCl concentrations, and (c) OECT related calibration curves. Nyquist plot toward different (d) KCl, (e) NaCl concentrations, and (f) EIS related calibration curves. R_W^* indicates intercept of the real component of the normalized impedance plot frequencies below 1 Hz. EIS performed at logarithmically spaced frequencies between 0.1 mHz and 10 kHz.

B. OECT Response

During the "dedoping process," due to the cations permeating in the channel with the positive gate voltage applied, a notable decrease in the magnitude of the drain current is visible. Consequently, an increase in the absolute value of the response was observed. The process reproducibility was investigated by channel resistance measurement ($R_{SD} = 1.67\,\text{k}\Omega \pm 81\,\Omega$), with an increase of ca. 6% post transfer. For both KCl and NaCl electrolyte solutions, the observed modulation in drain current was found to be directly proportional to the concentration of cation species present in the solution [see Fig. 3(a) and (b)]. This finding aligns with existing literature data [15], validating the consistency of our experimental results with established trends in the field. To asses the stability of the device, in the view of employing them as sensors, we repeated transfer characteristic (acquired every 10 min) in 0.1 MKCl. The result shown a good stability of the device with less than 4% changes between the previous measurements, indicating the applicability of the device as a sensor. In order to work before the saturation of the channel conductivity (estimated at $V_{off} = 0.85$ V), the relationship between device response and electrolyte solutions concentration at a fixed gate voltage 0.5 V was leveraged to establish a linear fitting, serving as a calibration curve Fig. 3(c). This calibration curve provides a quantitative framework for determining ion concentrations based on the observed device response, down to 1.25 mM, where the calibration curves intercept.

C. EIS Analysis

Analysis of the Nyquist plot, in Fig. 3(d) and (e), at high frequencies unveiled the expected decrease in the resistance of the electrolyte as the ion concentration increased, consistent for both NaCl and KCl electrolyte solutions, depicted by the decrease in diameter of the semicircle. This observation aligns with theoretical expectations, where a reduction in ion concentration leads to a higher resistance within the electrolyte. Notably, also the values of R_W^* extracted for both solutions demonstrated a clear proportional relationship with the ion concentration, as shown in Fig. 3(f), as R_W^* carries information about both ion concentration diffusion. In addition to this, comparing the extracted R_W^* for the two tested analytes, the values for the same concentration are higher in the case of NaCl solution. The relation from the experimental data $R^*_{W\,NaCl} > R^*_{W\,KCl}$ is in accordance with the principle of discrimination of ions based on their diffusion dynamics, considering both the mobility of ions $\mu_{Na^+} < \mu_{K^+}$ at 298 K [20] and the proportionality between diffusion $D \propto \mu$ [21] and $R_W^* \propto 1/cD$ [16], where c is the concentration of ions in the electrolyte.

D. 3-D Calibration Space

The calibration curves derived from the OECT response and EIS R_W^* against concentration do not intersect within the range between 1.25 and 100 mM, creating a 3-D calibration space as shown in Fig. 4(a). In particular OECT and EIS express higher sensitivity at high and low concentrations, respectively. This divergence highlights the distinct sensitivities of the two methods toward electrolyte components. On the other hand, through the combined utilization of both techniques, it becomes feasible to discern the two ion species, as well as their respective concentrations within an unknown electrolyte. As a numerical example, the OECT response for the 0.01 mM KCl solution is -0.75, but by using only the OECT measurement is not possible to distinguish the ion species, since the same response can be related to a 25 mM NaCl solution. Employing the EIS indicator $R_W^* = 0.4$ related to the 0.01 mM KCl, which in turn leads to the alternative electrolyte compositions 0.01 mM KCl or 55 mM NaCl, it is possible to identify only one possible electrolyte fulfilling both conditions: OECT and EIS response. By leveraging the complementary information provided by OECT and EIS, a comprehensive understanding of the electrolytic composition can be attained.

IV. CONCLUSION

In this letter, we have successfully realized a wearable OECT-based sensor directly on a textile substrate, enabling selectivity without the employment of traditional membranes or recognition elements. Both methods enable to achieve high coefficient of correlation $R^2 = 89\%$ for OECT and above 94% for EIS, between response and concentration.

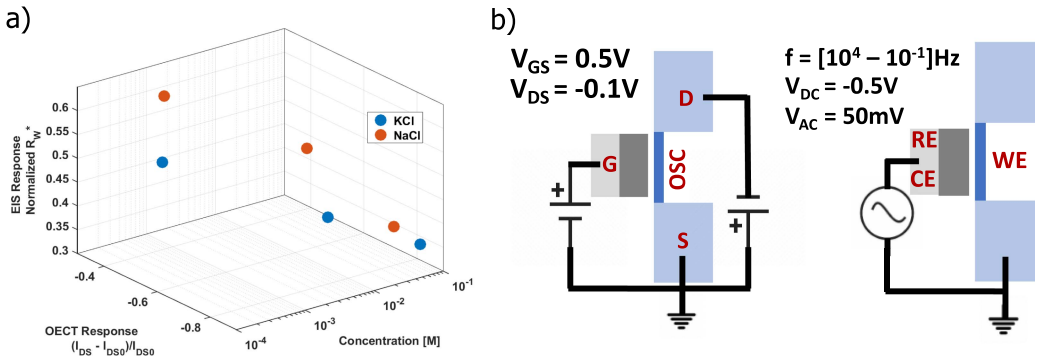

Fig. 4. (a) 3-D calibration space employing OECT response and EIS R_W and concentration. (b) Configuration of the device for both OECT and EIS measurement. OSC: organic semiconductor, G: gate, D: drain, S: source, WE: working electrode, RE: reference electrode, CE: counter electrode.

The electrochemical characterization of the PEDOT:PSS confirms that the mass transfer is controlled by diffusion. The device was characterized as both an OECT and as a two terminal EIS system, as described in Fig. 4(b) to extract the ion concentration and identify ion species in KCl and NaCl electrolytes, based on the combination of current response due to the PEDOT:PSS dedoping and the EIS response at low frequency representative of ion diffusion dynamics. The developed wearable OECT sensor on textile employed for EIS analysis holds promise for extension to encompass a broader array of ion species without dedicated membranes.

ACKNOWLEDGMENT

The views and opinions expressed are solely those of the authors and do not necessarily reflect those of the European Union, nor can the European Union be held responsible for them. This letter was supported in part by the European Union—NextGenerationEU under the National Recovery and Resilience Plan (PNRR), Mission 4 Component 2 Investment 1.3—Call for tender No. 341 of 15 March 2022, Italian Ministry of University and Research through Project code PE00000003, in part by the Italian Ministry of University and Research Concession Decree No. 1550 of 11 October 2022, through Project title "ON Foods - Research and innovation network on food and nutrition Sustainability, Safety and Security—Working ON Foods" and within the framework of the consortium iNEST - Interconnected Nord-Est Innovation Ecosystem (PNRR, Missione 4 Componente 2, Investimento 1.5 D.D. 1058 23/06/2022, ECS_00000043—Spoke1, RT2, CUP I43C22000250006), and in part by the Open Access Publishing Fund of the Free University of Bozen-Bolzano.

REFERENCES

[1] B. Shkodra et al., "Electrolyte-gated carbon nanotube field-effect transistor-based biosensors: Principles and applications," *Appl. Phys. Rev.*, vol. 8, no. 4, 2021, Art. no. 041325.

[2] Y. Li et al., "Ion-selective organic electrochemical transistors: Recent progress and challenges," *Small*, vol. 18, no. 19, 2022, Art. no. 2107413.

[3] X. Meng et al., "Selective ion sensing organic electrochemical transistors suitable for blood analysis," *Adv. Sensor Res.*, vol. 3, no. 1, 2024, Art. no. 2300097.

[4] M. Petrelli et al., "From rigid to flexible: Solution-processed carbon nanotube deposition on polymeric substrates for the fabrication of transistor-based ion sensors," *IEEE J. Flexible Electron.*, vol. 2, no. 4, pp. 300–307, Jul. 2023.

[5] M. Petrelli et al., "Flexible, planar, and stable electrolyte-gated carbon nanotube field-effect transistor-based sensor for ammonium detection in sweat," in *Proc. IEEE Int. Flexible Electron. Technol. Conf.*, 2022, pp. 1–2.

[6] M. Petrelli et al., "Method for instability compensation and detection of ammonium in sweat via conformal electrolyte-gated field-effect transistors," *Org. Electron.*, vol. 122, 2023, Art. no. 106889.

[7] R. Colucci, B. d. A. Feitosa, and G. C. Faria, "Impact of ionic species on the performance of PEDOT: PSS-based organic electrochemical transistors," *Adv. Electron. Mater.*, vol. 10, 2023, Art. no. 2300235.

[8] D. Majak, J. Fan, and M. Gupta, "Fully 3D printed oect based logic gate for detection of cation type and concentration," *Sensors Actuators B: Chem.*, vol. 286, pp. 111–118, 2019.

[9] S. Pecqueur, D. Guérin, D. Vuillaume, and F. Alibart, "Cation discrimination in organic electrochemical transistors by dual frequency sensing," *Org. Electron.*, vol. 57, pp. 232–238, 2018.

[10] H. Tseng, M. Cucchi, A. Weissbach, K. Leo, and H. Kleemann, "Membrane-free, selective ion sensing by combining organic electrochemical transistors and impedance analysis of ionic diffusion," *ACS Appl. Electron. Mater.*, vol. 3, no. 9, pp. 3898–3903, 2021.

[11] U. Boda, I. Petsagkourakis, V. Beni, P. A. Ersman, and K. Tybrandt, "Fully screen-printed stretchable organic electrochemical transistors," *Adv. Mater. Technol.*, vol. 8, 2023, Art. no. 2300247.

[12] M. A. C. Angeli et al., "Wearable sensors for non-invasive sport monitoring: An overview of the STEX project," in *Proc. IEEE Int. Flexible Electron. Technol. Conf.*, 2023, pp. 1–3.

[13] B. Shkodra et al., "A PEDOT: PSS/SWCNT-coated screen printed immunosensor for histamine detection in food samples," in *Proc. IEEE Int. Symp. Circuits Syst.*, 2020, pp. 1–4.

[14] J. Bobacka, A. Lewenstam, and A. Ivaska, "Electrochemical impedance spectroscopy of oxidized poly (3, 4-ethylenedioxythiophene) film electrodes in aqueous solutions," *J. Electroanalytical Chem.*, vol. 489, no. 1/2, pp. 17–27, 2000.

[15] N. Coppedè et al., "Ion selective textile organic electrochemical transistor for wearable sweat monitoring," *Org. Electron.*, vol. 78, 2020, Art. no. 105579.

[16] J. Bisquert, "Theory of the impedance of electron diffusion and recombination in a thin layer," *J. Phys. Chem. B*, vol. 106, no. 2, pp. 325–333, 2002.

[17] H. Yamada, K. Yoshii, M. Asahi, M. Chiku, and Y. Kitazumi, "Cyclic voltammetry part 2: Surface adsorption, electric double layer, and diffusion layer," *Electrochemistry*, vol. 90, no. 10, pp. 102006–102006, 2022.

[18] R. G. Compton and C. E. Banks, *Understanding Voltammetry*. Singapore: World Sci., 2018.

[19] X. Zheng, L. Li, L. Zhang, L. Xie, X. Song, and J. Yu, "Multiple self-cleaning paper-based electrochemical ratiometric biosensor based on the inner reference probe and exonuclease iii-assisted signal amplification strategy," *Biosensors Bioelectron.*, vol. 147, 2020, Art. no. 111769.

[20] P. W. Atkins, J. D. Paula, and J. Keeler, *Atkins' Physical Chemistry*. London, U.K.: Oxford Univ. Press, 2023.

[21] T. Bandara and B. Mellander, "Evaluation of mobility, diffusion coefficient and density of charge carriers in ionic liquids and novel electrolytes based on a new model for dielectric response," *Ionic Liquids: Theory, Properties, New Approaches*, vol. 17, no. 1, pp. 383–406, 2011.

Open Access funding provided by 'Libera Università di Bolzano' within the CRUI CARE Agreement